

# A review of the discrete element method/modelling in agricultural engineering

Qing Guo,<sup>1,2</sup> Huihuang Xia<sup>3</sup>

<sup>1</sup>Public Inspection and Testing Center, Hejiang County, Luzhou, China; <sup>2</sup>Quality Supervision and Inspection Center for Selenium-rich and Zinc-rich Products of Sichuan Province, Hejiang County, Luzhou, China; <sup>3</sup>Institute for Applied Materials (IAM), Karlsruhe Institute of Technology (KIT), Eggenstein-Leopoldshafen, Germany

## Abstract

With the development of high-performance computing technology, the number of scientific publications regarding computational modelling of applications with the Discrete Element Method/Modelling (DEM) approaches in agricultural engineering has risen in the past decades. Many granular materials, *e.g.* grains, fruits and soils in agricultural engineering are processed, and thus a better understanding of these granular media with DEM is of great significance in design and optimization of tools and process in agricultural engineering. In this review, the theory and background of DEM have been introduced. Some improved contact models discussed in the literature for accurately predicting the contact force between two interacting particles have been compared. Accurate approximation of irregular particle shapes is of great importance in DEM simulations to model real particles in agricultural engineering. New algorithms to approximate irregular particle shapes, *e.g.* overlapping multi-sphere approach, ellipsoid, *etc.*, have been summarized. Some remarkable engineering applications of the improved

numerical models developed and implemented in DEM are discussed. Finally, potential applications of DEM and some suggested further works are addressed in the last section of this review.

## Introduction

The Discrete Element Method/Modelling (DEM) is a numerical technique proposed by Cundall and Strack (1979), which has been widely used to model and understand the behavior of granular materials during the past decades. Xia *et al.* proposed an approach coupling DEM to the Finite Element Method (FEM) to understand the impact-induced deformation of screen mesh and the numerical approach developed in this work can be used to optimize the screen machines (Xia *et al.*, 2017). Another application of DEM is to model the screening process for a linear screening machine, and the underlining physics regarding particle looseness has been investigated (Li *et al.*, 2016; Wu *et al.*, 2018). An optimization algorithm has been developed by Chen *et al.* to optimize the elliptically vibrating screen, and discrete element simulations have been used to model the virtual screening process to validate the prediction of the hybrid MACO-GBDT algorithm (Chen *et al.*, 2021). In addition to these applications in processing engineering, DEM can also be used to model complex mechanical behavior in geotechnical engineering, *e.g.* Xia *et al.* investigated the crushing of brittle materials with an extended DEM and three different particle packing patterns (Xia *et al.*, 2019). DEM is also widely used in understanding complex physics in chemical engineering, *e.g.* modeling viscosity of particle suspensions (Kroupa *et al.*, 2016), aggregation of suspended micro-sized particles (Peng *et al.*, 2010), and various forces due to, *e.g.* DLVO theory, Brownian motion and Hooke's law implemented in DEM are used to model the agglomeration of polymer particles (Kroupa *et al.*, 2012). A more general and comprehensive review can be found in Zhu *et al.* (2008).

Particle shape is of great significance in the motion and contact behavior of granular media (Coetzee, 2016; Lu and McDowell, 2007). In agriculture, many irregular particle shapes, such as bulk wheat particles, corn kernel and soil powders can be found. In recent years, both conventional and extended DEM approaches have been increasingly used in agriculture to model and investigate various processes involving granular materials, such as soil (Qi *et al.*, 2019; Huang *et al.*, 2023), seeds (Pasha *et al.*, 2016), and fertilizers (Bangura *et al.*, 2020). The effect of particle shape on the seed motion and mixing has been investigated by Pasha *et al.* (2016). The X-ray microtomography was used to scan the surface of natural seeds (as shown in Figure 1) and then approximate the shape of real seeds with a certain number of overlapping spheres with different diameters, as shown in Figure 2.

The main focus of this review is to summarize the recent significant progress of these applications of DEM in modelling and optimizing some critical processes in agriculture. One of the primary applications of DEM in agriculture is to model the complex

Correspondence: Huihuang Xia, Institute for Applied Materials (IAM), Karlsruhe Institute of Technology (KIT), Hermann-von Helmholtz-Platz 1, 76344 Eggenstein-Leopoldshafen, Germany.  
E-mail: huihuang.xia@kit.edu

Key words: DEM; granular materials; contact model; agricultural engineering; contact force; particle shape.

Acknowledgments: we sincerely thank the insightful suggestions and comments on refining the contents of this review from Dr. Zhiqian Chen (Southeast University).

Conflict of interest: the authors declare no potential conflict of interest.

Received: 24 May 2023.  
Accepted: 20 June 2023.  
Early view: 4 August 2023.

©Copyright: the Author(s), 2023  
Licensee PAGEPress, Italy  
Journal of Agricultural Engineering 2023; LIV:1534  
doi:10.4081/jae.2023.1534

This work is licensed under a Creative Commons Attribution-NonCommercial 4.0 International License (CC BY-NC 4.0).

Publisher's note: all claims expressed in this article are solely those of the authors and do not necessarily represent those of their affiliated organizations, or those of the publisher, the editors and the reviewers. Any product that may be evaluated in this article or claim that may be made by its manufacturer is not guaranteed or endorsed by the publisher.

behavior of soil particles. Soil is a typical granular media with irregular particle shape, poly-disperse radius ratio, and different compositions, as shown in Figure 3. Understanding the behavior of soil particles is of great importance in designing and optimizing high-performance soil-engaging tools in agriculture as presented in Qi *et al.* (2019). The flowability of soil powders was modelled via DEM, and this numerical model was validated with experimental studies. It is found that the diameter of soil particles influences the kinetic energy of particles significantly. However, particle diameter has less influence on the angle of repose in these numerical simulations as found in this literature (Qi *et al.*, 2019).

Another promising application of numerical approaches based on DEM in agriculture is the computational modelling of seed particles. Seed particle is another typical granular material widely processed in agriculture. The mechanical behavior of seed particles can be influenced by various factors, *e.g.* particle shape (either convex or concave), moisture, and some other physical properties (Zhou *et al.*, 2020). In agricultural engineering, one goal is to disperse seeds efficiently and accurately. The DEM method can be used to model the dispersal of seeds, which is an essential process in crop production. For instance, DEM simulations can be used to study the effect of pressure airflow on the transport of seeds in the seed tube (Lu *et al.*, 2022; Schramm & Tekeste, 2022; Sharaby *et al.*, 2022). A summary of promising applications of numerical methods and models based on DEM is outlined in Table 1.

## Theory and mathematical formulation

The underlying physics behind DEM is governed by Newton's and Euler's second law of motion for translational and rotational motions, respectively.



**Figure 1.** Surface morphology of a natural corn seed particle obtained by the X-ray microtomography (Pasha *et al.*, 2016).

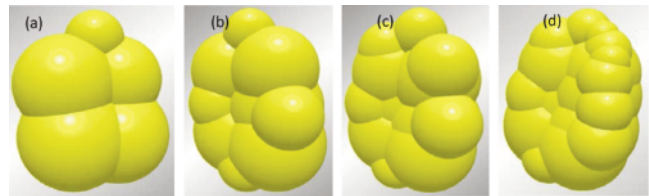


**Figure 2.** Representation of a real corn seed with overlapping sub-spheres in Discrete Element Method/Modelling with: (a) five, (b) ten, (c) fifteen and (d) twenty overlapping sub-spheres (Pasha *et al.*, 2016).



**Figure 3.** (a) A cylinder filled with soil particles is used to measure the angle of repose, (b) accumulations of soil particles on a wall (Qi *et al.*, 2019).

**Table 1.** Summary of remarkable applications of Discrete Element Method/Modelling approaches in engineering.

Authors (publication year)	Applications
Lu and McDowell (2007)	Effect of particle shape on heterogeneous stresses
Peng <i>et al.</i> (2010)	Aggregation of suspended nanoparticles
Kroupa <i>et al.</i> (2012)	Agglomeration of polymer particles
Li <i>et al.</i> (2016)	Particle looseness in screening process
Kroupa <i>et al.</i> (2016)	Viscosity in concentrated suspensions
Pasha <i>et al.</i> (2016)	Simulations of rotary seed coater
Xia <i>et al.</i> (2017)	DEM-FEM coupling for vibrating screen
Podlozhnyuk <i>et al.</i> (2017)	DEM simulations with superquadric particles
Soltanbeigi <i>et al.</i> (2018)	DEM simulations with irregular particles
Wu <i>et al.</i> (2018)	Parameter optimization of a linear vibrating screen
Qi <i>et al.</i> (2019)	Properties of soil flow
Xia <i>et al.</i> (2019)	Particle crushing and particle packing
Bangura <i>et al.</i> (2020)	Discharge of fertilizer particles
Chen <i>et al.</i> (2021)	Optimization of an elliptical vibrating screen
Schramm and Tekeste (2022)	Modelling flexible wheat straw
Lu <i>et al.</i> (2022)	Transport of seed particles in a tube
Sharaby <i>et al.</i> (2022)	Modelling sesame seed particles
Huang <i>et al.</i> (2023)	Movement of soil particles

These equations are given by

$$m_i \frac{d^2 x_i}{dt^2} = \sum_{j=1}^{N_p} F_{ij} + m_i g, \quad (1)$$

$$I_i \frac{d^2 \theta_i}{dt^2} = \sum_{j=1}^{N_p} M_{ij}. \quad (2)$$

Here, Eqn. 1 and Eqn. 2 are the governing equations for translational and rotational motions, respectively (Cundall and Strack, 1979). Additionally,  $m_i$  is the mass of the particle  $i$ ,  $N_p$  is the number of particles contacting with particle  $i$ , and  $F_{ij}$  is the interaction force acting on the particle  $i$  by its neighbouring particles interacting with it. In principle, the interaction force  $F_{ij}$  consists of two components, namely, forces in normal and tangential directions.  $F_{ij}$  is given by

$$F_{ij} = F_{ij}^n + F_{ij}^t, \quad (3)$$

where  $F_{ij}^n$  and  $F_{ij}^t$  are the interaction forces in normal and tangential directions, respectively (Goniva *et al.*, 2012; Norouzi *et al.*, 2016). The normal contact force  $F_{ij}^n$  is calculated by

$$F_{ij}^n = (k_n \delta_n - \gamma_n u_n^n) n_{ij}, \quad (4)$$

where  $n_{ij}$  is the unit normal vector pointing from particle  $i$  to particle  $j$ . Some other terms in Eqn. 4 are explained in the coming sections. Furthermore, the tangential contact force  $F_{ij}^t$  is computed by

$$F_{ij}^t = \min \left\{ \left| k_t \int_{t_0}^{t_c} u_t^r dt + \gamma_c u_t^r \right|, \mu_c F_{ij}^n \right\}, \quad (5)$$

where  $\mu_c$  is the coefficient of friction. This is the so-called history-dependent tangential contact force model which is implemented in the open-source DEM code LIGGGHTS (Computing, 2015).

In Eqn. 2,  $I_i$  is the moment of inertia of particle  $i$ ,  $\theta_i$  is the angular displacement of particle  $i$  and  $M_{ij}$  the moment acting on particle  $i$ . Numerical integration with the Verlet integration scheme (Verlet, 1967) is adopted to solve and update the particle position vector and angular displacement  $\theta_i$  from Eqs. 1 and 2. The numerical scheme to obtain and update the particle velocity  $u$  from Eqn. 1 is given by:

$$u \left( t + \frac{\Delta t}{2} \right) = u(t) + \frac{\Delta t}{2} \frac{du(t)}{dt}, \quad (6)$$

$$x(t + \Delta t) = x(t) + \Delta t u \left( t + \frac{\Delta t}{2} \right), \quad (7)$$

$$u(t + \Delta t) = u \left( t + \frac{\Delta t}{2} \right) + \frac{\Delta t}{2} \frac{du \left( t + \frac{\Delta t}{2} \right)}{dt}, \quad (8)$$

where  $\Delta t$  is the size of the time step. For such an explicit numerical scheme, the maximum time-step size must be smaller than the Rayleigh time-step size  $R_{ts}$  calculated by

$$R_{ts} = \frac{\pi \bar{R} \sqrt{\frac{2 \rho_p (1+\nu)}{E}}}{0.1631 \nu + 0.8766}, \quad (9)$$

where  $\bar{R}$  is the average particle radius,  $\rho_p$  the particle density,  $E$  the Young's modulus and  $\nu$  the Poisson's ratio (Norouzi *et al.*, 2016).

In addition to the second-order velocity Verlet integration scheme, the other two integration schemes are introduced for completeness. The first-order Euler integration scheme (also called the forward Euler method) is simple and easy to implement. It can also be used to update particle position and velocity. The basic idea for updating particle position and velocity is given by

$$x(t + \Delta t) = x(t) + u(t) \Delta t, \quad (10)$$

and

$$u(t + \Delta t) = u(t) + \frac{du(t)}{dt} \Delta t, \quad (11)$$

respectively (Atkinson, 1991).

The Leapfrog integration scheme is another second-order scheme, and it is a variant of the Verlet integration scheme. In Leapfrog integration scheme (Skeel, 1993), the position and velocity are updated by

$$x \left( t + \frac{\Delta t}{2} \right) = x(t) + u(t) \frac{\Delta t}{2}, \quad (12)$$

$$u(t + \Delta t) = u(t) + \frac{du \left( t + \frac{\Delta t}{2} \right)}{dt} \Delta t, \quad (13)$$

$$x(t + \Delta t) = x \left( t + \frac{\Delta t}{2} \right) + u \left( t + \Delta t \right) \frac{\Delta t}{2}. \quad (14)$$

More detailed discussion regarding these contact models in Eqs. 1 and 2 and numerical details can be found in the literature (Goniva *et al.*, 2012; Blais *et al.*, 2016; Norouzi *et al.*, 2016). During the past several decades, some open-source and commercial software have been developed for conducting DEM simulations. These software and code are listed in Table 2. Table 2 provides valuable guidance for engineers to select code/software for conducting DEM simulations.

**Table 2.** Summary of the open-source and commercial software/code for Discrete Element Method/Modelling simulations.

Code/Software	Parallel	Open-source	Description
LIGGGHTS	MPI	Yes	Modified from the open-source code LAMMPS
EDEM	Shared memory	No	Commercial code, can be coupled to Adams, Ansys, <i>etc.</i>
PFC	Multi-threaded	No	Commercial code, can conduct 2D and 3D simulations
Yade	OpenMP	Yes	Can be coupled to OpenFOAM, Escript, <i>etc.</i>
ESyS-Particle	MPI	Yes	Can be coupled to Escript, <i>etc.</i>
MFiX-DEM	MPI	Yes	Can be coupled to fluid simulation code
Woo	MPI	Yes	A fork of Yade DEM code
GranOO	OpenMP	Yes	Excellent in the bonded particle model
MercuryDPM	MPI	Yes	Large simulations with wide size distributions
BECKER 3D	MPI	No	Multiphase simulations with GPU acceleration

## Model development and applications

During the past decades, many promising applications regarding the understanding of processes in agricultural engineering have been presented in the literature. In this section, these applications are classified into the following subsections: contact models and algorithms for DEM, approximations of irregular natural seed particle shapes, and fancy applications of DEM in optimizing the design of tools for agricultural engineering.

### Contact models and algorithms for Discrete Element Method/Modelling

The contact model is of great significance in accurately predicting contact forces between two particles or a particle and a wall. During the past few years, several improved contact models have been developed for calculating contact forces accurately and accelerating numerical calculations. The Hertzian contact model is a simple yet efficient contact model to compute the contact force between two particles (Goodier and Timoshenko, 1970). The normal contact force  $F_n$  is given by

$$F_n = k_n \Delta x^3 \tag{15}$$

where  $\Delta x$  is the normal overlap between two particles, and  $k_n$  is the spring stiffness.  $k_n$  is calculated by

$$k_n = \frac{4}{3} E^* \sqrt{R^*} \tag{16}$$

where  $E^*$  and  $R^*$  the equivalent Young's modulus and radius, respectively. The two quantities are given by

$$E^* = \frac{E_i E_j}{E_i(1-\nu_j^2) + E_j(1-\nu_i^2)} \tag{17}$$

and

$$R^* = \frac{R_i R_j}{R_i + R_j} \tag{18}$$

respectively (with  $E_i$ ,  $R_i$ , and  $\nu_i$  being the Young's modulus, radius and Poisson's ratio of particle  $i$ , respectively). The hertzian contact model only accounts for the contribution of the spring model as shown in Eqn. 15. Visco-elastic contact model is extended to model the visco-elastic behavior of two interacting particles by adding the contribution of a dash-pot. The normal contact force calculated by the visco-elastic contact model is given by

$$F_n = k_n \Delta x^3 + c k_n \Delta x^\alpha U_n \tag{19}$$

where  $c$  is the damping coefficient of the dash-pot,  $\alpha$  is the exponent ( $\alpha$  can be 0.5 as suggested in the literature) and  $U_n$  is the relative velocity in the normal direction (Kuwabara and Kono, 1987; Seville *et al.*, 2000). Additionally, the first force term in Eqn. 19 is due to the elastic deformation between two particles, and the second term is non-linear and known as the viscous dissipative force term. Regarding the damping coefficient in the visco-elastic model, it is defined by

$$c = 2K^* \sqrt{R^*} \tag{20}$$

where  $K^*$  is the equivalent curvature of two interacting particles

whose curvatures  $K_i$  and  $K_j$ , respectively.

Thornton and Ning proposed an adhesive contact model to model the stick/bounce behavior of granular media (Thornton and Ning, 1998). The force-displacement relationship is demonstrated in Figure 4, and the detailed derivation of this model can be found via (Thornton and Ning, 1998; Horabik and Molenda, 2016).

Luding (2008) proposed a very simple contact model for cohesive and frictional granular materials in the range of 0.1-10  $\mu\text{m}$ . This model is known as the adhesive and elastic-plastic contact model, and the force-displacement relationship can be found in Figure 5. The contact force of the adhesive and elastic-plastic Luding model is given by

$$f_{\text{hys}} = \begin{cases} k_1 \delta, & \text{if } k_2(\delta - \delta_0) \geq k_1 \delta, \\ k_2(\delta - \delta_0), & \text{if } k_1 \delta > k_2(\delta - \delta_0) > -k_c \delta, \\ -k_c \delta, & \text{if } -k_c \delta \geq k_2(\delta - \delta_0). \end{cases} \tag{21}$$

In addition to these aforementioned contact models for calculating the contact force. In DEM, another promising model called the Bounded Particle Model (BPM) has been used to model continuous media within the framework of DEM. The basic idea of BPM is to generate virtual beams for every particle-particle pair and set parameters for beams. These beams fail and break when external forces acting on beams are larger than their strength threshold. A simple BPM implemented in the open-source DEM code YADE was conducted by Xia *et al.* to model the continuous media, namely, a rectangular rock sample and its crushing behavior was numerically investigated (Xia *et al.*, 2019). In agricultural engineering, the BPM is extended to model the failure of flexible straw stems by Shi *et al.* (2023). In this study, two different types of virtual bonds have been proposed, as shown in Figure 6. Simulation results are found to be

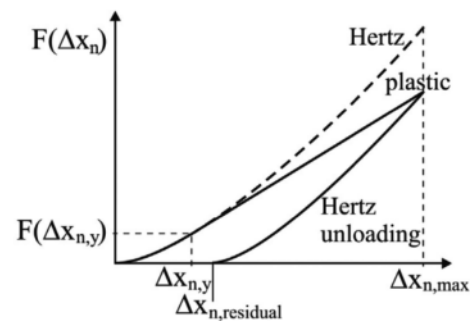


Figure 4. Force versus displacement of the Thornton model (Horabik and Molenda, 2016).

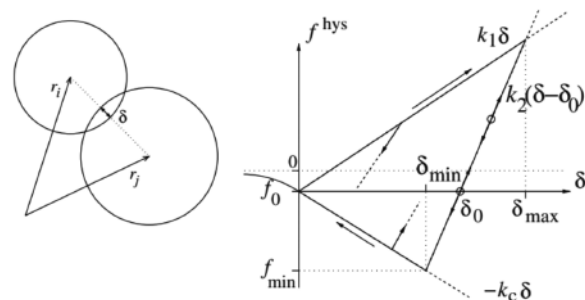
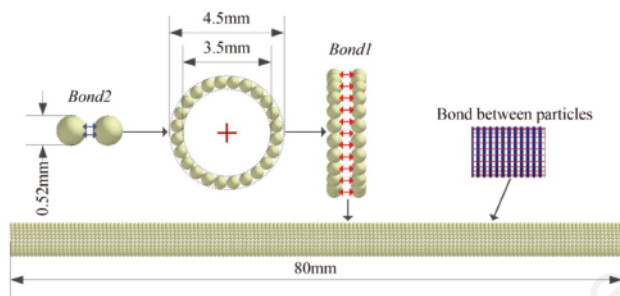


Figure 5. Left image: two interacting particles with overlap  $\delta$ ; Right image: force-displacement diagram (Luding, 2008).

in good agreement with corresponding experimental validations. It proves that the BMP proposed by Shi (2023) is feasible and promising in modelling flexible straw steams. Another remarkable study conducted by Wang *et al.* (2019) investigates the effect of particle size ranging from 3 to 19 mm on soil-subsoiler interactions with a Hertz-Mindlin Bonding (HMB) model implemented in the commercial DEM software EDEM. In this study, soil rupture distance ratio, height of accumulated soil, and soil disturbance area were investigated by varying the particle radius. It found that particles with a radius of 7 mm are recommended for numerical simulations with the HMB model (Wang *et al.*, 2019). An extended Hertz-Mindlin model with the bonding contact was developed by Zhao *et al.* (2023) for modelling the cotton stalk as shown in Figure 7. The experimental study was used to validate the bonded model implemented in EDEM and found that the Hertz-Mindlin model with bonding contact is suitable for modelling the cotton stalk (Zhao *et al.*, 2023).

A better understanding of the tensile behaviour of tobacco leaf

is of importance to design and optimize tobacco harvesting machines. An extended DEM model with virtual bonds was proposed to model the flexible tobacco leaf under tensile conditions as shown in Figure 8. The particle packing pattern does influence the mechanical behaviour of the continuous media, as discussed in the literature (Xia *et al.*, 2019). As shown in the magnified sub-figure of Figure 8, the packing pattern is the so-called modified hexagonal close packing with some initial gap between every two particles. Additionally, simple cubic packing and some other packing patterns can also be used for the bonded particle model. In this study, two different regions, namely, a non-linear region and an elastic region have been found. This numerical model successfully predicted both the general trend and the data-yielding elastic behaviour (Tian *et al.*, 2023; Ucgul & Saunders, 2020). A brief summary of these aforementioned contact models are outlined in Table 3.



**Figure 6.** The schematic diagram of modelling a flexible straw steam with Discrete Element Method/Modelling (Shi *et al.*, 2023).

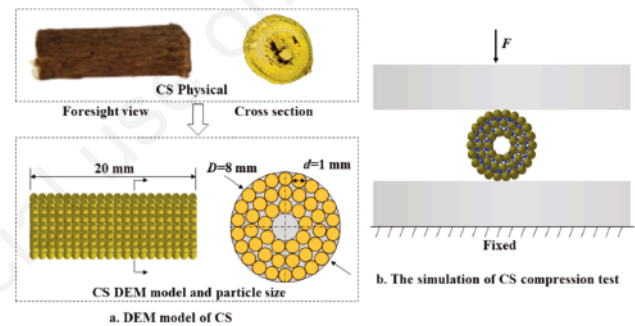


**Figure 7.** (a) numerical approximation of a cotton stalk in Discrete Element Method/Modelling; (b) the numerical set-up of the compression test (Zhao *et al.*, 2023).

**Table 3.** Summary of contact models in Discrete Element Method/Modelling.

Authors (publication year)	Formula/Applications
Goodier and Timoshenko (1970)	$F_n = \frac{4}{3} E^* \sqrt{R^*} \Delta x^{\frac{3}{2}}$
Kuwabara Kuwabara and Kono (1987)	$F_n = k_n \Delta x^{\frac{3}{2}} + c k_n \Delta x^\alpha U_n$
Luding (2008)	$f_{nys} = \begin{cases} k_1 \delta, & \text{if } k_2(\delta - \delta_0) \geq k_1 \delta, \\ k_2(\delta - \delta_0), & \text{if } k_1 \delta > k_2(\delta - \delta_0) > -k_c \delta, \\ -k_c \delta, & \text{if } -k_c \delta \geq k_2(\delta - \delta_0). \end{cases}$
Xia <i>et al.</i> (2019)	Crushing of rock samples
Wang <i>et al.</i> (2019)	Soil-subsoiler interactions
Ucgul and Saunders (2020)	Soil-mouldboard plough interaction
Zhao <i>et al.</i> (2023)	Compression test of the cotton
Shi <i>et al.</i> (2023)	Stalk flexible straw steams
Tian <i>et al.</i> (2023)	Tensile behaviour of tobacco leaf

## When particle shape matters

Accurate approximations of natural seed shapes are of great importance in the computational modelling of complex behavior of seed particles with DEM.

Constructing the irregular particles with several overlapping spheres has been adopted in the literature (Lu and McDowell, 2007; Wang *et al.*, 2018; Song *et al.*, 2021). Lu and McDowell proposed a simple procedure to represent real ballast particles by clumping some overlapping spheres together, as shown in Figure 9. The approximation of real ballast particles depends on the number of sub-spheres used to generate the clumps; namely, more particles guarantee a smooth representation of ballast particles (Lu and McDowell, 2007; Soltanbeigi *et al.*, 2018). Several numerical approaches have been proposed to model irregular seed particles with DEM. Zhou *et al.* (2020) proposed four different filling methods, namely horse-tooth shape, truncated triangular pyramid shape, ellipsoid cone shape, and spheroid shape for approximating maize seed particles as shown in Figures 10 and 11. Approximating the irregular shape of seed particles with clump methods as presented in Lu and McDowell (2007), Wang *et al.*, (2018), and Zhou *et al.* (2020), leads to coarse surface roughness. An improved approach called spherical harmonics was proposed by Radvilaitė *et al.* (2016) to model three different agricultural grains, namely, bean, chickpea, and maize. The main finding of this study is that a proper combination of low- and high-resolution harmonics can accurately represent either concave or convex shapes of particles. Li *et al.* (2022a) used the rapid prototyping method to model the corn kernel particle, and this new method was proved to have a better representation of four common particle shapes, *e.g.* corn kernel, corncob, garlic, and wheat. The shape of wheat seeds does influence the complex behavior of seed particles and the accuracy of the numerical model. A robust and accurate ellipsoid modelling approach was proposed by Lu *et al.* (2023). The general formula of the ellipsoid method for generating the ellipsoidal particles is given by

$$f(x, y, z) = \left( \frac{|x|^t}{|a|^t} + \frac{|y|^t}{|b|^t} \right)^r + \frac{|z|^t}{|c|^t} - 1 = 0, \quad (22)$$

where  $a$ ,  $b$ , and  $c$  are the half-lengths along the coordinate axes, respectively. Additionally,  $t$  and  $r$  represent the sharpness indices of the particle surface (Lu *et al.*, 2023). The comparison between numerical simulations with ellipsoids and simulations with irregular particles constructed with multi-sphere approaches (Xu *et al.*, 2018; Binelo *et al.*, 2019; Li *et al.*, 2022b; Kafashan *et al.*, 2021;

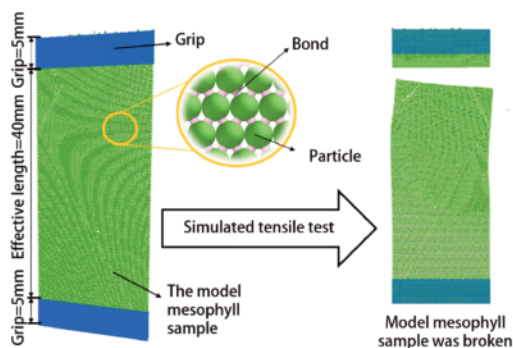


**Figure 8.** The numerical set-up for Discrete Element Method/Modelling simulations of the tensile test (Tian *et al.*, 2023).

Wang *et al.*, 2022a; Boac *et al.*, 2023) proves that the ellipsoid method is more accurate in representing the particle shape.

Contact detection is of great importance in DEM simulations, especially for simulations with non-spherical particles as contact detection consumes the majority of computational time for a DEM simulation. The bounding volume method, namely, using a simple volume to encapsulate a more complex body (shown in Figure 12) was adopted by Podlozhnyuk *et al.* (2017) to reduce the number of detected potential contact pairs in a neighbor list. Once the contact pairs are detected, the next step is to further detect every contact for every two superquadrics. The so-called “midway” approach was developed by Soltanbeigi *et al.* (2018) to conduct the contact detection for superquadrics.

The basic idea is shown in Figure 13. Two superquadrics with

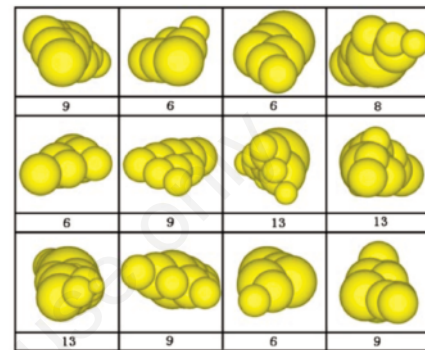


**Figure 9.** Constructions of irregular particles with overlapping spheres as clumps (Lu and McDowell, 2007).

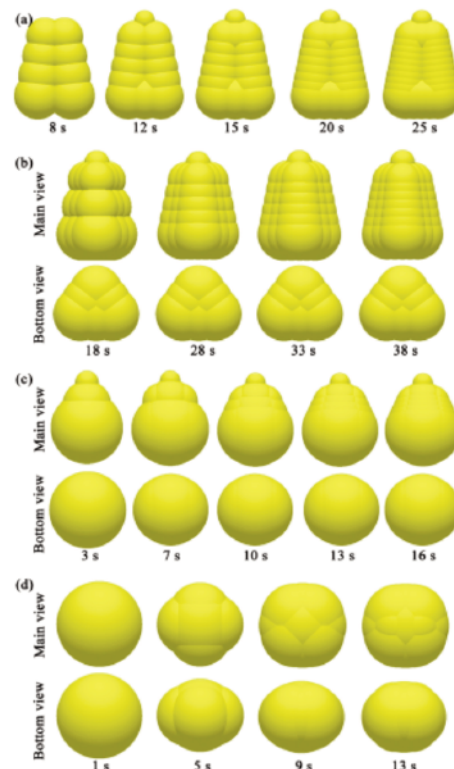


**Figure 10.** Constructions of irregular particles with overlapping spheres with four different methods: (a) horse-tooth shape; (b) truncated triangular pyramid shape; (c) ellipsoid cone shape; (d) spheroid shape (Zhou *et al.*, 2020).

centroids denoted by  $X_{CA}$  and  $X_{CB}$ , respectively. This algorithm is to find the midpoint denoted as  $X_0$  between two intersection points  $X_A$  and  $X_B$ . More detailed numerical issues and algorithms can be found in the literature (Podlozhnyuk *et al.*, 2017; Soltanbeigi *et al.*, 2018).

## Modelling particle-tool interactions by Discrete Element Method/Modelling

In addition to these extended contact models and algorithms to approximate the complex irregular particle shape mentioned in the previous sections, some promising applications of DEM in agricultural engineering are discussed in this section.

Contact and interactions with neighbouring apples may lead to mechanical injury in the form of bruise damage when handling apples. A visco-elastic model has been developed and adopted for modelling bruise formations of apples which are approximated by the multi-sphere model as shown in Figure 14 (Scheffler *et al.*, 2018). The agreement between the real shape of an apple and the numerical approximation becomes better by increasing the angle of smoothness. It demonstrates that this model can predict the dynamic bulk behaviour and mean bruise damage of an apple.

Understanding tool-particle interactions is of great significance in the optimization of tools used in agricultural engineering. DEM can capture the complex interactions between two particles, and a particle interacting with an agricultural tool. The influence of moisture contents, namely 7.5%, 21.5% and 38% on the traction force when modelling shoe-soil interactions with DEM was investigated by Shaikh *et al.* (2021).

The numerical error of around 10.09% is found when comparing numerical results obtained with the EDEM software against the experimental data. The complex motion of agricultural particles on the screen surface was numerically modelled by DEM in the literature (Ma *et al.*, 2015; 2017). A variable-amplitude screening model was developed to understand the migration and dispersion of particles during the screening process. The main conclusion is that the frequency and turning angle influence the expansion of agricultural particles (Ma *et al.*, 2017). Modelling cohesive soil particles with the hysteretic spring contact model coupling to the linear cohesion model, and the movement of tools on these cohesive soil beds was computationally modelled with DEM (Aikins *et al.*, 2021). The motion patterns and dynamic response characteristics of sunflower seed particles were investigated by Wang *et al.* (2022b), and the multi-sphere approach was used to represent the real sunflower seed particle as shown in Figure 15. The accuracy in approximating the shape of the sunflower seed is improved by increasing the number of sub-particles.

It turns out that the surface roughness of the numerical sunflower seed particles influences the accuracy of the numerical model, and a rough surface leads to poor simulation results (Wang *et al.*, 2022b).

## Summary and outlook

In this review, the application of the discrete element method in agricultural engineering during the past few years has been summarized. DEM is a promising numerical approach in modelling different irregular agricultural particles, *e.g.* wheat kernel, corn, apple, strawberry, *etc.* The multi-sphere approach, rapid prototype technology and ellipsoid approach have been used to approximate irregular particles. The existing contact models in DEM can be used to model the flow and cohesion of agricultural particles. The

BMP has been used to model continuous and flexible agricultural particles, such as cotton stalks and tobacco leaves.

For future work, some potential applications and opening of the DEM method are outlined below:

- Approximations of natural agricultural particles. As seen in the most recent literature, superquadrics have been adopted in DEM to model irregular granular materials. Superquadric particles can be used to model a wide range of particle shapes, and this approach can be used to approximate many irregular agricultural particles.
- New contact models for very fine particles. Some non-contacting forces, *e.g.* Van der Waals force and electrostatic force can

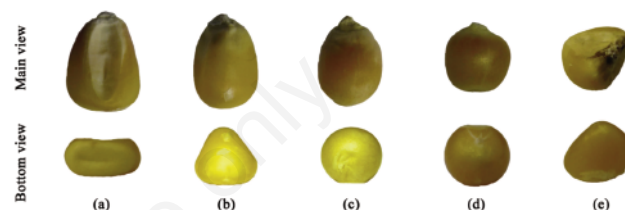


**Figure 11.** Different particle shapes of maize seeds: (a) horse-tooth shape, (b) truncated triangular pyramid shape, (c) ellipsoid cone shape, (d) spheroid shape and (e) irregular shape (Zhou *et al.*, 2020).

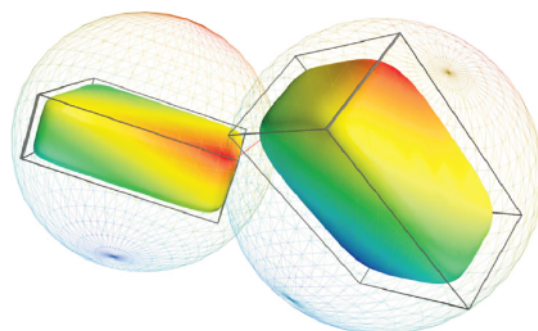


**Figure 12.** Schematic diagram of bounding spheres and oriented bounding boxes for superquadrics (Podlozhnyuk *et al.*, 2017).

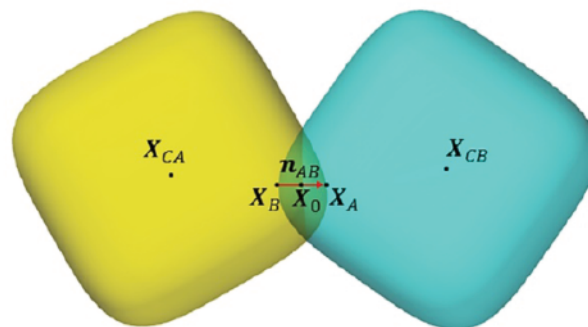


**Figure 13.** Schematic diagram of particle-particle contact for superquadrics (Soltanbeigi *et al.*, 2018).

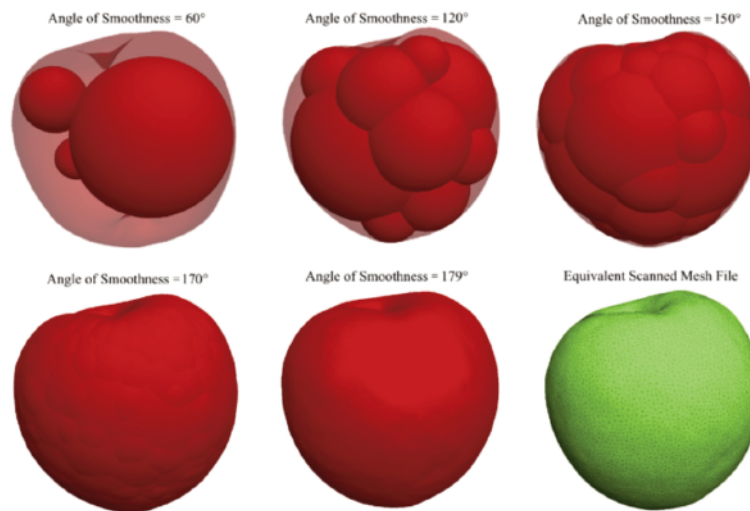


**Figure 14.** The effect of the angle of smoothness on approximations of a real apple with overlapping sub-particles (Scheffler *et al.*, 2018).

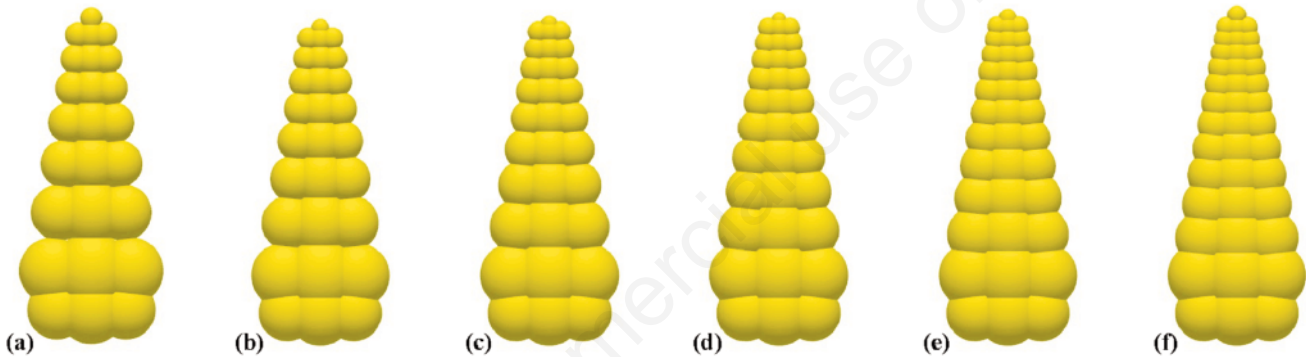


**Figure 15.** Representation of the sunflower seed with multi-sphere approach in Discrete Element Method/Modelling: (a) 25, (b) 28, (c) 31, (d) 34, (e) 37, (f) 40 sub-spheres (Wang *et al.*, 2022b).

not be negligible when the size of particles becomes smaller (*e.g.*, in micro-scale). In agricultural engineering, flour powders are widely processed. Modelling micro-sized flour powders with DEM can be enhanced by incorporating the non-contact Van der Waals force.

- Liquid bridge force model for long-range interactions. Granular materials containing some liquids demonstrate different behavior from that of dry granular materials. Incorporating the liquid bridge model can be very helpful in further understanding the liquid-bridge-induced cohesion of agricultural particles.
- Coupling to some other numerical methods. DEM has been reported to couple to FEM for modelling contact-induced deformation, abrasion, *etc.* Computational Fluid Dynamics (CFD) has been extensively used to model compressive fluid in agricultural engineering. Accordingly, coupling DEM to CFD for modelling the gas-flow-induced motion of solid particles can be an interesting topic.
- GPU-based parallel computations for large-scale simulations. In agricultural engineering, large amounts of solid granular particles are processed. The scaling method has been proposed in the literature to scale the numerical model and to reduce the

computational cost. The GPU-based parallel computational approach can be used to accelerate these computations when processing a considerable amount of irregular agricultural particles.

- Biologically inspired engineering. Biologically inspired structures have been used in mechanical engineering to enhance the mechanical properties under dynamic loads, *e.g.* energy absorption, lightweight structures, and the joint design Siddique *et al.* (2022), Zhang *et al.* (2022), Xu *et al.* (2022), Marquez-Florez *et al.* (2023). Accordingly, some structures from nature can inspire the design of some tools in agricultural engineering. Design and optimization of these biological-inspired structures and tools can be conducted with extensive DEM simulations.

## References

- Aikins K.A., Ucgul M., Barr J.B., Jensen T.A., Antille D.L., Desbiolles J.M.A. 2021. Determination of discrete element model parameters for a cohesive soil and validation through narrow point opener performance analysis. *Soil Tillage Res.*

- 213:105123.
- Atkinson K. 1991. An introduction to numerical analysis. John Wiley & sons.
- Bangura K., Gong H., Deng R., Tao M., Liu C., Cai Y., Liao K., Liu J., Qi L. 2020. Simulation analysis of fertilizer discharge process using the discrete element method (DEM). *PloS one* 15:e0235872.
- Binelo M.O., de Lima R.F., Khatchatourian O.A., Stránský J. 2019. Modelling of the drag force of agricultural seeds applied to the discrete element method. *Biosyst. Eng.* 178:168-75.
- Blais B., Lassaingne M., Goniva C., Fradette L., Bertrand F. 2016. Development of an unresolved CFD-DEM model for the flow of viscous suspensions and its application to solid-liquid mixing. *J Comput. Phys.* 318:201-21.
- Boac J.M., Casada M.E., Pordesimo L.O., Petingco M.C., Maghirang R.G., Harner III J.P. 2023. Evaluation of particle models of corn kernels for discrete element method simulation of shelled corn mass flow. *Smart Agric. Technol.* 4:100197.
- Chen Z., Li Z., Xia H., Tong X. 2021. Performance optimization of the elliptically vibrating screen with a hybrid MACO-GBDT algorithm. *Particuology* 56:193-206.
- Coetzee C.J. 2016. Calibration of the discrete element method and the effect of particle shape. *Powder Technol.* 297:50-70.
- Cundall P.A., Strack O.D.L. 1979. A discrete numerical model for granular assemblies. *Géotechnique* 29:47-65.
- DCS Computing. LIGGGHTS-DEM simulation engine, 2015. Available from: <https://github.com/CFDEMproject/LIGGGHTS-PUBLIC>
- Goniva C., Kloss C., Deen N.G., Kuipers J.A.M., Pirker S. 2012. Influence of rolling friction on single spout fluidized bed simulation. *Particuology* 10:582-91.
- Goodier J.N., Timoshenko S. 1970. Theory of elasticity. McGraw-Hill.
- Horabik J., Molenda M. 2016. Parameters and contact models for DEM simulations of agricultural granular materials: A review. *Biosyst. Eng.* 147:206-25.
- Huang S., Lu C., Li H., He J., Wang Q., Cao X., Gao Z., Wang Z., Lin H. 2023. Research on acoustic wave attenuation from the perspective of soil particle movement using the discrete element method. *Comput. Electron. Agric.* 207:107747.
- Kafashan J., Wiacek J., Ramon H., Mouazen A.M. 2021. Modelling and simulation of fruit drop tests by discrete element method. *Biosyst. Eng.* 212:228-240.
- Kroupa M., Klejch M., Vonka M., Kosek J. 2012. Discrete element modeling (DEM) of agglomeration of polymer particles. *Procedia Eng.* 42:58-69.
- Kroupa M., Vonka M., Soos M., Kosek J. 2016. Utilizing the discrete element method for the modeling of viscosity in concentrated suspensions. *Langmuir* 32:8451-60.
- Kuwabara G., Kono K. 1987. Restitution coefficient in a collision between two spheres. *Jpn. J. Appl. Phys.* 26:1230.
- Li A., Jia F., Wang Y., Han Y., Chen P., Zhang J., Fei J., Shen S., Hao X., Feng W. 2022b. Numerical analysis of the rice transport uniformity in vertical friction rice mill based on discrete element method. *Comput. Electron. Agric.* 202:107398.
- Li X., Du Y., Liu L., Mao E., Wu J., Zhang Y., Guo D. 2022a. A rapid prototyping method for crop models using the discrete element method. *Comput. Electron. Agric.* 203:107451.
- Li Z., Tong X., Xia H., Yu L. 2016. A study of particles looseness in screening process of a linear vibrating screen. *J. Vibroeng.* 18:671-81.
- Lu B., Ni X., Li S., Li K., Qi Q. 2022. Simulation and experimental study of a split high-speed precision seeding system. *Agriculture* 12:1037.
- Lu C., Gao Z., Li H., He J., Wang Q., Wei X., Wang X., Jiang S., Xu J., He D., Li Y. 2023. An ellipsoid modelling method for discrete element simulation of wheat seeds. *Biosyst. Eng.* 226:1-15.
- Lu M.M.G.R., McDowell G.R. 2007. The importance of modelling ballast particle shape in the discrete element method. *Granul. Matter* 9:69-80.
- Luding S. 2008. Cohesive, frictional powders: contact models for tension. *Granul. Matter* 10:235-46.
- Ma Z., Li Y., Xu L. 2015. Discrete-element method simulation of agricultural particles' motion in variable-amplitude screen box. *Comput. Electron. Agric.* 118:92-9.
- Ma Z., Li Y., Xu L., Chen J., Zhao Z., Tang Z. 2017. Dispersion and migration of agricultural particles in a variable-amplitude screen box based on the discrete element method. *Comput. Electron. Agric.* 142:173-80.
- Marquez-Florez K., Arroyave-Tobón S., Linares J.M. 2023. From biological morphogenesis to engineering joint design: a bio-inspired algorithm. *Mater. Des.* 225:111466.
- Norouzi H.R., Zarghami R., Sotudeh-Gharebagh R., Mostoufi N. 2016. Coupled CFD-DEM modeling: formulation, implementation and application to multiphase flows. John Wiley & Sons.
- Pasha M., Hare C., Ghadiri M., Gunadi A., Piccione P.M. 2016. Effect of particle shape on flow in discrete element method simulation of a rotary batch seed coater. *Powder Technol.* 296:29-36.
- Peng Z., Doroodchi E., Evans G. 2010. DEM simulation of aggregation of suspended nanoparticles. *Powder Technol.* 204:91-102.
- Podlozhnyuk A., Pirker S., Kloss C. 2017. Efficient implementation of superquadric particles in discrete element method within an open-source framework. *Comput. Part. Mech.* 4:101-18.
- Qi L., Chen Y., Sadek M. 2019. Simulations of soil flow properties using the discrete element method (DEM). *Comput. Electron. Agric.* 157:254-60.
- Radvilaitė U., Ramírez-Gómez A., Kačianauskas R. 2016. Determining the shape of agricultural materials using spherical harmonics. *Comput. Electron. Agric.* 128:160-71.
- Scheffler O.C., Coetzee C.J., Opara U.L. 2018. A discrete element model (DEM) for predicting apple damage during handling. *Biosyst. Eng.* 172:29-48.
- Schramm M., Tekeste M.Z. 2022. Wheat straw direct shear simulation using discrete element method of fibrous bonded model. *Biosyst. Eng.* 213:1-12.
- Seville J.P.K., Willett C.D., Knight P.C. 2000. Interparticle forces in fluidisation: a review. *Powder Technol.* 113:261-8.
- Shaikh S.A., Li Y., Ma Z., Chandio F.A., Hussain Tunio M., Liang Z., Solangi K.A. 2021. Discrete element method (DEM) simulation of single grouser shoe-soil interaction at varied moisture contents. *Comput. Electron. Agric.* 191:106538.
- Sharaby N., Doroshenko A., Butovchenko A. 2022. Modelling and verification of sesame seed particles using the discrete element method. *J. Agric. Eng.* 53.
- Shi Y., Jiang Y., Wang X., Thuy N.T.D., Yu H. 2023. A mechanical model of single wheat straw with failure characteristics based on discrete element method. *Biosyst. Eng.* 230:1-15.
- Siddique S.H., Hazell P.J., Wang H., Escobedo J.P., Ameri A.A.H. 2022. Lessons from nature: 3D printed bio-inspired porous structures for impact energy absorption—a review. *Addit. Manuf.* p103051.
- Skeel R.D. 1993. Variable step size destabilizes the störmer/leapfrog/verlet method. *BIT Numer. Math.* 33:172-5.
- Soltanbeigi B., Podlozhnyuk A., Papanicolopu-los S.-A., Kloss C., Pirker S., Ooi J.Y. 2018. DEM study of mechanical characteristics of multi-spherical and superquadric particles at micro and macro scales. *Powder Technol.* 329:288-303.

- Song W., Xu F., Wu H., Xu Z. 2021. Investigating the skeleton behaviors of open-graded friction course using discrete element method. *Powder Technol.* 385:528-36.
- Thornton C., Ning Z. 1998. A theoretical model for the stick/bounce behaviour of adhesive, elastic-plastic spheres. *Powder Technol.* 99:154-62.
- Tian Y., Zeng Z., Gong H., Zhou Y., Qi L., Zhen W. 2023. Simulation of tensile behavior of tobacco leaf using the discrete element method (DEM). *Comput. Electron. Agric.* 205:107570.
- Ucgul M., Saunders C. 2020. Simulation of tillage forces and furrow profile during soil-mouldboard plough interaction using discrete element modelling. *Biosyst. Eng.* 190:58-70.
- Verlet L. 1967. Computer "experiments" on classical fluids. I. thermodynamical properties of Lennard-Jones molecules. *Phys. Rev.* 159:98.
- Wang J., Xu C., Xu W., Fu Z., Wang Q., Tang H. 2022a. Discrete element method simulation of rice grain motion during discharge with an auger operated at various inclinations. *Biosyst. Eng.* 223:97-115.
- Wang S., Yu Z., Aorigele, Zhang W. 2022b. Study on the modeling method of sunflower seed particles based on the discrete element method. *Comput. Electron. Agric.* 198:107012.
- Wang X., Li Z., Tong X., Ge X. 2018. The influence of particle shape on screening: Case studies regarding DEM simulations. *Eng. Comput.*
- Wang X., Zhang S., Pan H., Zheng Z., Huang Y., Zhu R. 2019. Effect of soil particle size on soil-subsoiler interactions using the discrete element method simulations. *Biosyst. Eng.* 182:138-50.
- Wu X., Li Z., Xia H., Tong X. 2018. Vibration parameter optimization of a linear vibrating banana screen using DEM 3D simulation. *J. Eng. Technol. Sci.* 50.
- Xia H., Li Z., Tong X. 2019. Modelling continuous materials using discrete element modelling: investigations on the effect of particle packing. *Comput. Part. Mech.* 6:823-36.
- Xia H., Tong X., Li Z., Wu X. 2017. DEM-FEM coupling simulations of the interactions between particles and screen surface of vibrating screen. *Int. J. Min. Miner. Eng.* 8:250-63.
- Xu T., Yu J., Yu Y., Wang Y. 2018. A modelling and verification approach for soybean seed particles using the discrete element method. *Adv. Powder Technol.* 29:3274-90.
- Xu X., Zhang Y., Wang X., Fang J., Chen J., Li J. 2022. Searching superior crashworthiness performance by constructing variable thickness honeycombs with biomimetic cells. *Int. J. Mech. Sci.* 235:107718.
- Zhang Y., Xu X., Fang J., Huang W., Wang J. 2022. Load characteristics of triangular honeycomb structures with self-similar hierarchical features. *Eng. Struct.* 257:114114.
- Zhao W., Chen M., Xie J., Cao S., Wu A., Wang Z. 2023. Discrete element modeling and physical experiment re-search on the biomechanical properties of cotton stalk. *Comput. Electron. Agric.* 204:107502.
- Zhou L., Yu J., Wang Y., Yan D., Yu Y. 2020. A study on the modelling method of maize-seed particles based on the discrete element method. *Powder Technol.* 374:353-76.
- Zhu H.P., Zhou Z.Y., Yang R.Y., Yu A.B. 2008. Discrete particle simulation of particulate systems: a review of major applications and findings. *Chem. Eng. Sci.* 63:5728-70.